Proc. Natl. Acad. Sci. USA
Vol. 92, pp. 8846–8850, September 1995
Biophysics

The three-dimensional structure of NAD(P)H:quinone reductase, a flavoprotein involved in cancer chemoprotection and chemotherapy: Mechanism of the two-electron reduction

(x-ray diffraction/flavin)

RONGBAO LI*, MARIO A. BIANCHET*, PAUL TALALAY†, AND L. MARIO AMZEL*‡

*Department of Biophysics and Biophysical Chemistry, and †Department of Pharmacology and Molecular Sciences, Johns Hopkins University School of Medicine, Baltimore, MD 21205

Contributed by Paul Talalay, May 11, 1995

ABSTRACT **Quinone reductase [NAD(P)H:(quinone acceptor) oxidoreductase, EC 1.6.99.2], also called DT diaphorase, is a homodimeric FAD-containing enzyme that catalyzes obligatory NAD(P)H-dependent two-electron reductions of quinones and protects cells against the toxic and neoplastic effects of free radicals and reactive oxygen species arising from one-electron reductions. These two-electron reductions participate in the reductive bioactivation of cancer chemotherapeutic agents such as mitomycin C in tumor cells. Thus, surprisingly, the same enzymatic reaction that protects normal cells activates cytotoxic drugs used in cancer chemotherapy. The 2.1-Å crystal structure of rat liver quinone reductase reveals that the folding of a portion of each monomer is similar to that of flavodoxin, a bacterial FMN-containing protein. Two additional portions of the polypeptide chains are involved in dimerization and in formation of the two identical catalytic sites to which both monomers contribute. The crystallographic structures of two FAD-containing enzyme complexes (one containing $NADP^+$, the other containing duroquinone) suggest that direct hydride transfers from NAD(P)H to FAD and from $FADH_2$ to the quinone [which occupies the site vacated by NAD(P)H] provide a simple rationale for the obligatory two-electron reductions involving a ping-pong mechanism.**

Quinone reductase [NAD(P)H:(quinone acceptor) oxidoreductase, EC 1.6.99.2, QR] is a widely distributed FAD-containing protein (1, 2) that catalyzes nicotinamide nucleotide-dependent reductions of quinones, quinoneimines, azo dyes, and nitro groups (2). Induction of QR (3, 4) protects against the toxic and neoplastic effects of quinones. Measurement of inducer potency has been used to isolate anticarcinogens (5) and to design chemoprotectors (6). Protection by QR is conferred by catalysis of obligatory two-electron reductions (7) that divert quinones from redox cycling, from reacting with critical nucleophiles, and from depleting sulfhydryl groups (4, 8). QR also reductively activates important chemotherapeutic quinones such as mitomycins and aziridylbenzoquinones (9). Thus, since levels of QR are often elevated in tumors, the selective susceptibility of tumors to such agents (10, 11) provides the opportunity for designing improved chemotherapeutic agents that are more efficiently activated by QR (9).

QR has been crystallized from mouse and rat liver and the Walker rat tumor. Preliminary x-ray diffraction data have been reported (12–15). The catalytic properties (2, 15, 16), physiological functions (2), and transcriptional regulation of QR have been studied extensively (17, 18). QR is a dimer of identical subunits, each comprising 273 amino acids; the FAD prosthetic group in each subunit is noncovalently attached but remains bound during catalytic cycling; NADH or NADPH cycle in and out of the enzyme and must be released from the enzyme before substrate can bind; no products of one-electron reductions arise; the enzyme is inhibited by Cibacron blue (15, 19) and by dicumarol, warfarin, and other anticoagulants.§ Understanding the catalytic mechanism of QR requires detailed structural information, which is also crucial to clarifying the mechanism responsible for the obligatory two-electron reductions.

Table 1. X-ray data collection and analysis

Data set	Resolution, Å	Unique reflections,* no.	Completeness, %	R_{merge}†
Native				
Complex I‡	2.4	23,775 (2.3)	89.8	5.0
Complex II§	2.1	35,123 (4.5)	88.1	5.5
Derivative				
$Hg(CN)_2$	2.4	22,943 (2.2)	86.0	7.5
C_2H_5HgCl	2.4	23,593 (2.7)	87.9	6.0
K_2PtCl_4	2.4	18,959 (2.6)	85.6	6.0

*Numbers in parentheses, ratio of measurements to unique reflections.
†$R_{merge} = \Sigma_h\Sigma_i|I_{hi} - \langle I_h\rangle|/\Sigma_h\Sigma_i|I_{hi}|$, $\langle I\rangle$ average intensity from multiple measurements.
‡Complex I: QR complex with FAD, Cibacron blue, and duroquinone.
§Complex II: QR complex with FAD and $NADP^+$.

We have determined the crystal structure of rat liver QR by x-ray diffraction to 2.1-Å resolution (Tables 1–3).¶ Structures were determined and refined for two FAD-containing complexes of the same crystal form (I2): complex I, containing Cibacron blue (a potent inhibitor) and tetramethyl-1,4-benzoquinone (duroquinone); and complex II, containing $NADP^+$.

MATERIALS AND METHODS

QR was purified from rat livers by Cibacron blue affinity chromatography (15). Crystals were obtained by the hanging drop method. Protein solutions (≈10 mg/ml) were equilibrated by vapor diffusion and crystals were grown from solutions containing 1.45 M ammonium sulfate, 0.5% polyethylene glycol 8000, 30 mM Cibacron blue [pure ring A *o*-sulfonate (19)], and 150 mM imidazole (pH 7.0). These crystals belong to space group $P2_1$ and contain four monomers

The publication costs of this article were defrayed in part by page charge payment. This article must therefore be hereby marked "*advertisement*" in accordance with 18 U.S.C. §1734 solely to indicate this fact.

Abbreviation: QR, quinone reductase.
‡To whom reprint requests should be addressed.
§In addition to roles in cancer chemoprotection and chemotherapy, QR may reduce vitamin K oxide as part of the coagulation cascade (20). Inhibition by dicumarol and warfarin suggests that the QR structure may be used to design more effective anticoagulants.
¶The atomic coordinates and structure factors have been deposited in the Protein Data Bank, Chemistry Department, Brookhaven National Laboratory, Upton, NY 11973 (reference 1QRD).

Table 2. Phasing statistics

Derivative	Isomorphous difference,* %	$R_{centric}$†	Phasing power‡
$Hg(CN)_2$ (1.0 mM, 32 days)	20.0	0.52	2.1
C_2H_5HgCl (saturated, 20 days)	25.0	0.61	1.8
K_2PtCl_4 (1.0 mM, 18 days)	12.4	0.88	0.7

The average figure of merit of the multiple isomorphous replacement phases is 0.61.

*Mean fractional isomorphous difference = $\Sigma_h|F_{PH} - F_P|/\Sigma_h|F_P|$, where F_P = protein structure factor amplitude, F_{PH} = heavy atom derivative structure factor amplitude.

†$R_{centric} = \Sigma_h|(|F_{PH} - F_P| - |f_H|)|/\Sigma_h|F_{PH} - F_P|$, for centric reflections, where f_H = heavy atom structure factor amplitude.

‡Phasing power = $(|f_H|/E)_{rms}$, where E = residual lack of closure error.

in the asymmetric unit (13). The I2 crystal form used in all studies (a = 72.0 Å, b = 107.0 Å, c = 88.4 Å, β = 92.6°), containing two monomers in the asymmetric unit, was obtained by soaking $P2_1$ crystals in 2.8–3.0 M ammonium succinate containing 60 mM duroquinone (complex I). Soaking complex I crystals in 2.8–3.0 M ammonium succinate with 10 mM $NADP^+$, in the absence of Cibacron blue or duroquinone, provided complex II. Heavy atom derivatives were prepared by soaking crystals in mother liquors containing 1 mM heavy atom compounds (Table 1). Data were collected with a Siemens multiwire area detector with CuKα radiation from a Rigaku rotating anode generator with a graphite monochromator. Frames were integrated and scaled by XDS (21, 22). Derivative and native data, as well as most of the multiple isomorphous replacement calculations, were carried out with CCP4 (23). Solvent flattening was performed with the package of Wang (24) and map averaging and phase combination with an in-house program (25). Models were built with the programs "O" (26) and CHAIN (27) on Silicon Graphics Workstations. Structures were refined using X-PLOR (28) (Table 3). Color figures were drawn with SETOR (29).

RESULTS AND DISCUSSION

Overall Structure. The two monomers in the asymmetric unit of rat liver QR crystals (I2 form) are related by a local two-fold axis of symmetry but unexpectedly do not constitute the physiological dimer. The latter is formed by two monomers related by a crystallographic two-fold axis of symmetry.

Each subunit contains two separate domains: a major, catalytic domain (residues 1–220) folded in a predominantly α/β structure and a small, C-terminal domain (residues 221–273) (Fig. 1). The two-domain structure is compatible with proteolytic digestion experiments (30). The overall folding of the catalytic domain resembles that of other flavoproteins: a

Table 3. Refinement statistics

	Complex I	Complex II
Reflections	21,737 (6.0 to 2.4 Å, $F > 2\sigma_F$)	31,541 (6.0 to 2.1 Å, $F > 2\sigma_F$)
Non-hydrogen atoms	4,612	4,612
Solvent atoms	48	48
R value	0.189	0.199
Average B factor	20.0 Å^2	24.0 Å^2
Deviation from ideality		
Bond lengths	0.018 Å	0.017 Å
Bond angles	3.12°	3.08°
Improper torsions	2.86°	2.05°

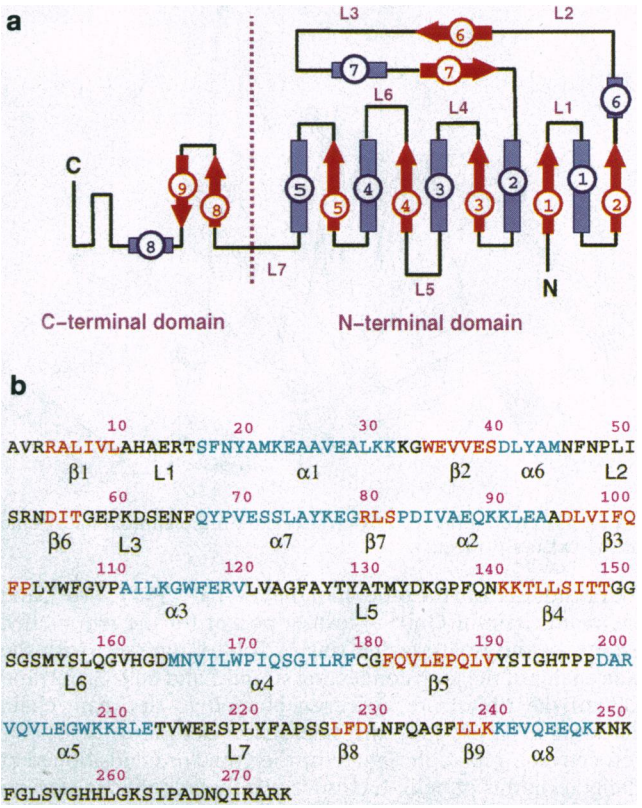

FIG. 1. Secondary structure elements of quinone reductase. (*a*) α-Helices, blue rectangles; β-sheets, red arrows; loops, black lines. Helices and strands are numbered as in *Clostridium* flavodoxin; additional helices and strands are labeled consecutively starting at 6. (*b*) Elements of secondary structure are color coded: strands, red; α-helices, blue; loops, black.

twisted central parallel β-sheet surrounded on both sides by connecting helices (Fig. 2). The C-terminal domain contains an antiparallel hairpin motif followed by one helix and several loops. Surprisingly, the exact topology of the catalytic domain differs from that found in other FAD-containing proteins but resembles the topology of *Clostridium* flavodoxin (31), an FMN-containing protein without significant sequence identity.‖ When the structures of QR and *Clostridium* flavodoxin are aligned, 80 α-carbons superimpose with an rms deviation of 1.8 Å between the two molecules (program ALIGN; ref. 32). Within this portion of the structure, QR has a 40- to 45-residue insertion comprising a β–α–β motif that connects strand 2 to helix 2, which are directly connected in flavodoxin (31).

FAD Binding Site. The positions of the flavin in QR and in *Clostridium* flavodoxin are similar. The isoalloxazine moiety interacts with residues in loops at one end of the molecule (L1 and L4 of one monomer and L3 and L5 of the other monomer). The aromatic residues Tyr^{104}, Trp^{105}, Phe^{106}, and the main chain of Leu^{103} interact directly with the rings and anchor the isoalloxazine moiety. The two oxygen atoms of the flavin ring (O2F and O4F)** form hydrogen bonds with main chain NH groups of the protein: O4 with Phe^{106} and O2 with Gly^{150} (Fig. 3). The ring nitrogens also form hydrogen bonds with NH groups of the protein: N1F with Gly^{149} and N5F with Trp^{105}. Two residues from one monomer—Tyr^{104} and Trp^{105}—and

‖Since the ping-pong mechanism requires binding of flavin and either NAD(P)H or substrate, QR resembles electron carriers like flavodoxin rather than those flavoenzymes that simultaneously bind both nicotinamide nucleotides and substrates.

**The atoms in each portion of the cofactors are designated by letters that identify the ring to which they belong: F, flavin; A, adenosine of FAD; and N, nicotinamide-ribose.

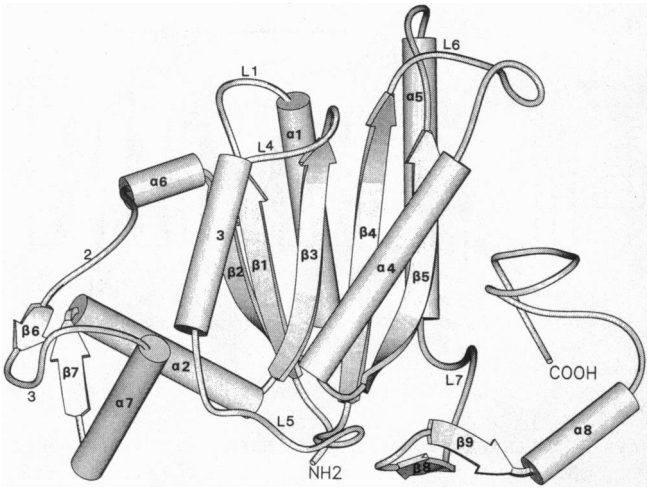

FIG. 2. Overall fold of QR projected onto the approximate plane of the twisted β-sheet.

four residues from the other monomer—Ile[50], Tyr[67], Pro[68], and the main chain of Glu[117]—form a pocket for the two methyl groups of the isoalloxazine ring.†† Ribitol interacts with the side chains of the loop connecting strand 3 and helix 3. O2′ and O3′ of the ribitol are hydrogen bonded to the main chain carbonyl of Leu[103] and the side chain OH group of Thr[147], respectively. The diphosphate of the cofactor is positioned at the N terminus of helix 1, close to the loop connecting strand 1 to helix 1. The two phosphates make several specific contacts with groups in the protein: OP1F forms a hydrogen bond with the main chain NH of Asp[18] at the N terminus of helix 1, and OP2F with the Nε of His[11]. A water molecule, hydrogen bonded to the OH of Tyr[104], makes hydrogen bonds with O3′F and OP2F. One oxygen atom of the adenine phosphate (OP1A) is hydrogen bonded to the Nε of Gln[66]. The ribose is bound by residues from helix 1 and by the loop connecting strand 1 to helix 1. The adenine ring lies along helix 5 and interacts most strongly with Arg[200]. N3A (i.e., of FAD adenine) forms a hydrogen bond with the guanidinium NH1 and the ring makes contacts with the main chain and with CH_2 groups of Arg[200]. It also interacts with the main chain of residues Thr[15], Ser[16], and Phe[17] and with the side chains of Ala[20] and Leu[204]. FAD has the same position in both complexes.

NADP⁺ Binding Site. In complex II, the nicotinamide of NADP⁺ and ring C of the isoalloxazine are stacked (Fig. 4), at an average distance between the planes of the two rings of about 3.4 Å. The binding site for NADP⁺ involves both residues of the same subunit that binds FAD and residues from the other subunit of the dimer. (This is one of the arguments used to identify the physiological dimer.) The carbonyl group of the nicotinamide (O7N) makes two hydrogen bonds: one with the OH of Tyr[126] and the other with the OH of Tyr[128] of the second monomer (Fig. 5). (More detailed analysis of $2F_o - F_c$ and $F_o - F_c$ maps suggests that the nicotinamide moiety in complex II also exists in a minor alternative conformation related by an 180° rotation around the bond between N1 of nicotinamide and C1 of ribose.) The side chain of Phe[178], also of the second monomer, stacks against the nicotinamide ring. The O2′N of the nicotinamide ribose makes a hydrogen bond with the Nε of His[161] and the C3′N is in van der Waals contact with the S of Met[154]. The O3′N appears to interact with the center of the aromatic ring of Tyr[128]. His[194] is positioned to form potential hydrogen bonds between its Nε atom and two oxygens of the diphosphate. The AMP moiety interacts mainly with the hairpin loop formed by strands 8 and 9 of the other monomer (Fig. 6): the ribose makes contacts with Phe[232] and Phe[236] and the adenine moiety with the main chain of residues in the loop. The main chain NH of Phe[232] forms a hydrogen bond with one of the oxygens of the phosphate at the O2′A

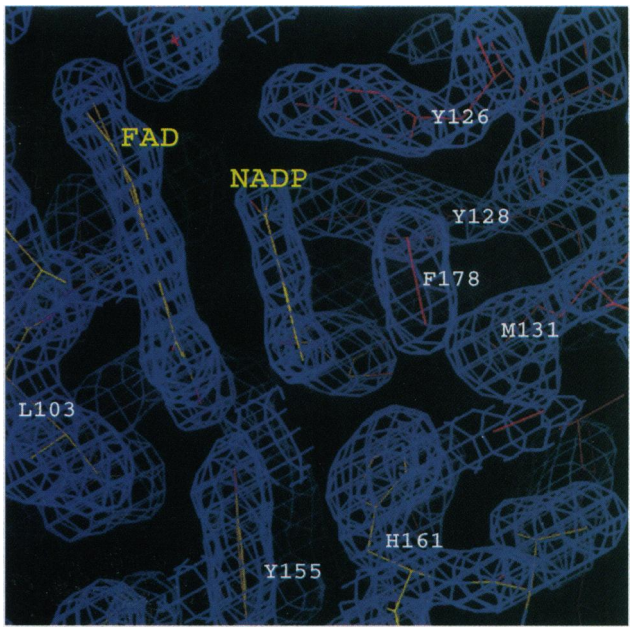

FIG. 4. Electron density of FAD and NADP⁺. Electron density 2 $F_o - F_c$ map in the region of the isoalloxazine and nicotinamide rings showing stacking of the rings and position of the F178 phenyl ring stacking on the other side of the nicotinamide.

††In mouse and human QR, Tyr[104] is replaced by glutamine, which is the only rat QR residue that contacts a ligand and is not conserved in other species (33).

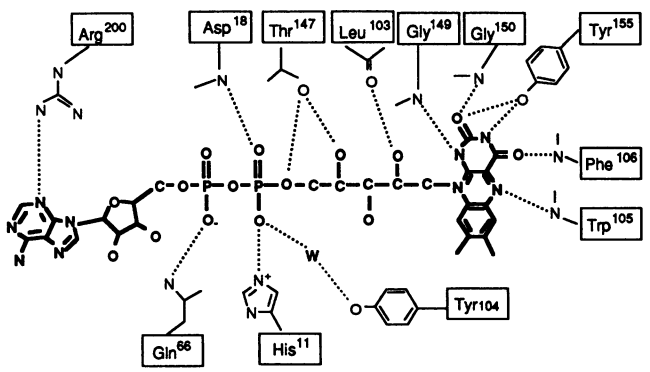

FIG. 3. Schematic representation of FAD/QR interactions, showing residues involved in hydrogen bonds to the cofactor. W, water.

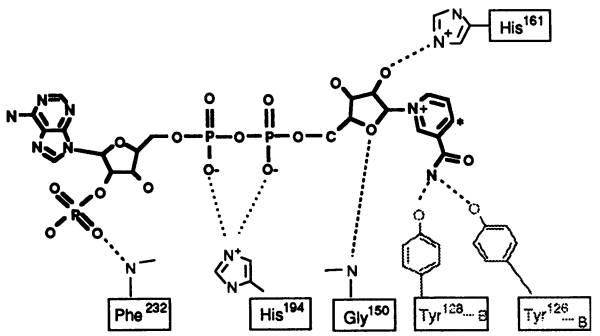

FIG. 5. Schematic representation of NADP⁺/QR interactions showing residues involved in hydrogen bonds to the cofactor.

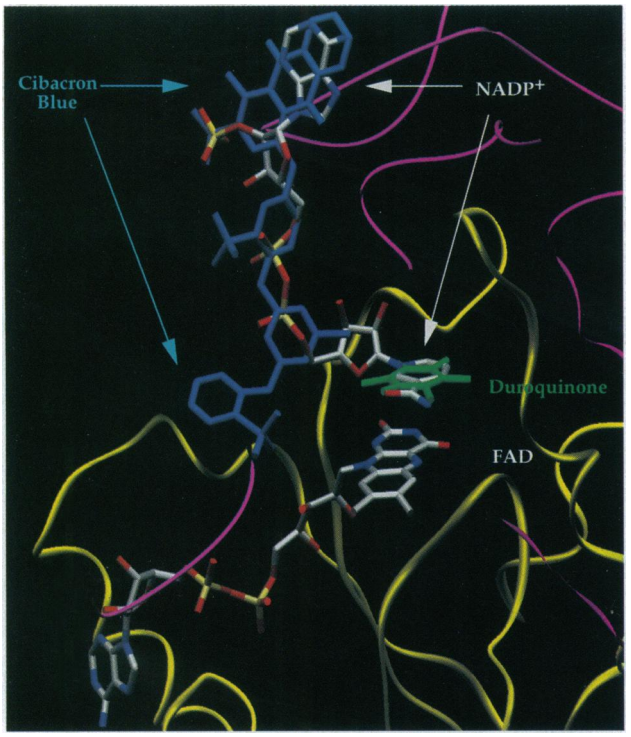

FIG. 6. Superposition of cofactor, inhibitor, and substrate (combined information from complexes I and II). FAD is bound in the same position in both complexes. $NADP^+$ (carbon, gray; oxygen, red; nitrogen, blue; phosphorous, yellow) is in the position found in complex II. Duroquinone (green) is in the position found in complex I; it fully overlaps the nicotinamide ring of $NADP^+$ in complex II. Cibacron blue (blue) is in the position found in complex I. Three of its four rings overlap the position of the ADP of $NADP^+$ found in complex II.

position of adenine ribose. This hydrogen bond is not present when NADH is the cofactor, which may explain the difference in affinities between NADH and NADPH (15). The sequence TTGGSGS (residues 147–153), which has been suggested as part of the NADH binding site (15, 34, 35), is not involved in any specific interactions with the dinucleotide, but the main chain of these residues is apparently packed very close to both cofactors: Gly^{149} interacts with one ribitol oxygen of FAD and makes a hydrogen bond with N1F, and Gly^{150} interacts with oxygen O4′N of the ribose adjacent to nicotinamide and with O2F of the flavin. Similar to other nucleotide binding proteins with this consensus sequence, the two glycines facilitate proximity of the main chain and cofactors.

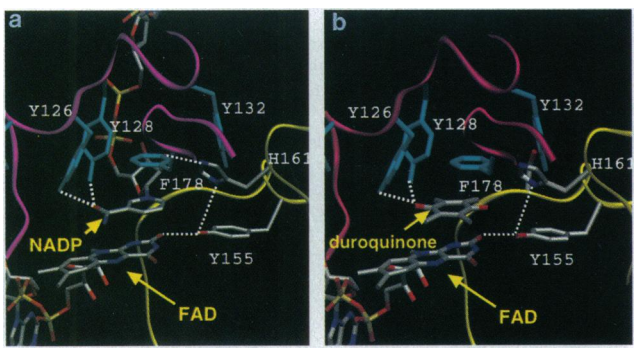

FIG. 7. Mechanism of quinone reductase. (*a*) Binding of $NADP^+$ to QR. The position of C4N of the nicotinamide is 4.0 Å from the N5F of the flavin. (*b*) Binding of duroquinone to QR. The quinone is in an optimal position to receive a hydride from the $FADH_2$ (FAD represented here).

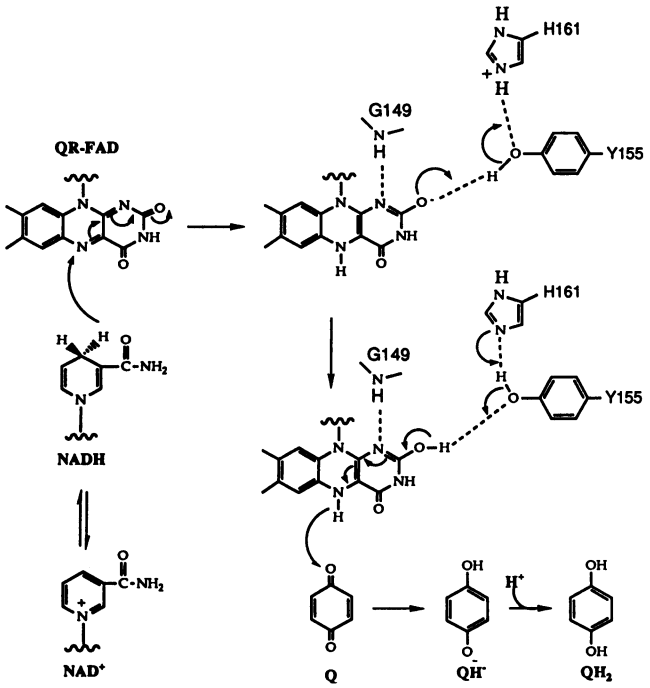

FIG. 8. Mechanism of the obligatory two-electron reduction of benzoquinone (Q) by QR. The overall reaction is: NADH + Q + H^+ → NAD^+ + QH_2.

Duroquinone (Tetramethyl-1,4-benzoquinone) and Cibacron Blue Binding Sites. In complex I, duroquinone (a substrate) occupies a position very similar to that of the nicotinamide ring of $NADP^+$ in complex II (Fig. 6). It stacks with the isoalloxazine ring (distance between the two rings, 3.4 Å) and one of its oxygens forms hydrogen bonds with the OH groups of Tyr^{126} and Tyr^{128}. Cibacron blue fully overlaps the position occupied by the rest of the $NADP^+$ (the ribose, phosphate, and adenosyl groups) in complex II but does not interfere with quinone binding. Cibacron blue and the AMP moiety of $NADP^+$ interact very similarly with the enzyme, as expected since the dye binds to proteins with nucleotide binding sites. Three of the ring systems of Cibacron blue (B, C, and D) play important roles in mimicking AMP binding‡‡ (Fig. 6). The observed binding explains the pattern of inhibition of QR by Cibacron blue: competitive with respect to NADH and noncompetitive with respect to quinone (15, 19).

Bound Conformations and Mechanism. If oxidized nicotinamide of $NADP^+$ is used to model the position of the ring in the reduced form, the structure is ideal for a direct hydride transfer from NAD(P)H to FAD, in the first half of the reaction cycle: C4 of the nicotinamide is 4.0 Å from N5 of flavin (Fig. 7*a*). The nicotinamide is in the *syn* conformation around the glycosidic bond, with the flavin stacking on its *endo* side (36). The isoalloxazine is in the *anti* conformation with the dimethylbenzene ring pointing away from the ribose. In this orientation the 4-*pro*-S hydrogen (B-side) of the reduced nicotinamide can be transferred as a hydride to the *re*-face of

‡‡In complex I, the anthraquinone ring (D; see ref. 19) of Cibacron blue occupies a position very similar to that of the adenine and ribose of $NADP^+$ in complex II: it interacts with the main chain of the loop connecting strands 8 and 9. The sulfonate of ring D makes a hydrogen bond to the NH of Phe^{232}. The NH connecting rings D and C is hydrogen bonded to the main chain NH of Tyr^{128}. The ring itself interacts with the side chains of Phe^{232} and Phe^{236}. The NH connecting ring C to ring B is hydrogen bonded to His^{194}. Ring B stacks on the side chain of Tyr^{126}. Ring A does not make contacts with the protein, consistent with inhibitor kinetics (19).

the flavin N5F.§§ As mentioned above, the N1F is hydrogen bonded to the NH of Gly^{149}. Since no groups can donate a proton to compensate a charge if it develops on N1F (as commonly proposed for other systems), the most likely tautomer is the enol form with the negative charge at O2F (Fig. 8). Because O2F is already the acceptor atom of a hydrogen bond with Tyr^{155}, this tautomer can receive the proton from the OH of Tyr^{155}, which can, in turn, be stabilized by the positive charge of (or the transfer of a proton from) His^{161} (Fig. 7*a*). Replacement of Tyr^{155} by site-directed mutagenesis produced mutant enzymes that showed decreased but still significant enzymatic activity (34). The imidazole of His^{161} is close to the nicotinamide (Fig. 7*a*), so the net effect of this step (in addition to transfer of the hydride from nicotinamide to isoalloxazine) is movement of a positive charge over a very short distance from the imidazole ring of His^{161} to the nicotinamide. This process is reversed when the hydride is transferred to the quinone.

Binding of substrate cannot occur until $NAD(P)^+$ is released because the quinone and the nicotinamide share the same site, thus accounting for the ping-pong mechanism. The quinone binds to the vacated site in an orientation ideally suited to accept a hydride from $FADH_2$ (Fig. 7*b*). The quinone is reduced by the hydride to the singly ionized hydroquinone (hydroquinolate), and the isoalloxazine is oxidized to the quinonoid form. The proton on O2F is transferred back to the OH of Tyr^{155}. The imidazole ring of His^{161} becomes fully protonated again and can either transfer a proton to the hydroquinolate or simply stabilize its negative charge (Fig. 8). In addition to hydride transfer, the second half of the reaction transfers a proton from the O2F (accepted in the first half of the reaction) to the hydroquinolate.

In conclusion, the structure clearly explains how QR promotes obligatory two-electron reductions: *both* halves of the reaction involve hydride transfers—first from NAD(P)H to FAD and then from $FADH_2$ to the quinone.¶¶ The charge relay formed by Tyr^{155} and His^{161} allows the reaction to take place without unfavorable charge separations.

§§Lee *et al.* (37) reported that the hydride transfer from NADH and NADPH by rat liver QR occurs with pro-4*R* (A-side) stereospecificity. This finding is only compatible with the alternative nicotinamide orientation (above), which may be catalytically competent.

¶¶This mechanism suggests that replacement of FAD by 5-deaza-FAD should retain enzymatic activity, in agreement with recent experiments (38). The transfer of a hydrogen atom followed by very rapid transfer of one electron is also possible.

We thank Dr. T. Prestera for help in protein purification and for a gift of pure Cibacron blue; Dr. J. C. Boyington and Dr. C. H. Robinson for many helpful discussions; Drs. X. Ysern, H. J. Prochaska, and S. Bedarkar, who contributed extensively to the initial stages of this work; and Drs. J. Wehrle and N. Carrasco for careful reading of the manuscript. This work was supported by National Institutes of Health Grants GM45540 (L.M.A.) and CA44530 (P.T.) and by equipment grants from the National Science Foundation, the National Institutes of Health, and the Lucille Markey Foundation.

1. Ernster, L. & Navazio, F. (1957) *Biochim. Biophys. Acta* **26,** 408–415.
2. Ernster, L., Estabrook, R. W., Hochstein, P. & Orrenius, S. (1987) *Chem. Scr.* **27,** 1–207.
3. Benson, A. M., Hunkeler, M. J. & Talalay, P. (1980) *Proc. Natl. Acad. Sci. USA* **77,** 5216–5220.
4. Prochaska, H. J. & Talalay, P. (1991) in *Oxidative Stress: Oxidants and Antioxidants*, ed. Sies, H. (Academic, London), pp. 195–211.
5. Zhang, Y., Talalay, P., Cho, C.-G. & Posner, G. H. (1992) *Proc. Natl. Acad. Sci. USA* **89,** 2399–2403.
6. Posner, G. H., Cho, C.-G., Green, J. V., Zhang, Y. & Talalay, P. (1994) *J. Med. Chem.* **37,** 170–176.
7. Iyanagi, T. & Yamazaki, I. (1970) *Biochim. Biophys. Acta* **216,** 282–294.
8. Talalay, P. (1989) *Adv. Enzyme Regul.* **28,** 237–250.
9. Ross, D., Siegel, D., Beall, H., Prakash, A. S., Mulcahy, R. T. & Gibson, N. W. (1993) *Cancer Metastasis Rev.* **12,** 83–101.
10. Schlager, J. J. & Powis, G. (1990) *Int. J. Cancer* **45,** 403–409.
11. Berger, M. S., Talcott, R. E., Rosenblum, M. L., Silva, M., Ali-Osman, F. & Smith, M. T. (1985) *J. Toxicol. Environ. Health* **16,** 713–719.
12. Amzel, L. M., Bryant, S. H., Prochaska, H. J. & Talalay, P. (1986) *J. Biol. Chem.* **262,** 1379.
13. Ysern, X. & Prochaska, H. J. (1989) *J. Biol. Chem.* **264,** 7765–7767.
14. Skelly, J. V., Suter, D. A., Knox, R. J., Garman, E., Stuart, D. I., Sanderson, M. R., Roberts, J. J. & Neidle, S. (1989) *J. Mol. Biol.* **205,** 623–624.
15. Prochaska, H. J. (1988) *Arch. Biochem. Biophys.* **267,** 529–538.
16. Hosoda, S., Nakamura, W. & Hayashi, K. (1974) *J. Biol. Chem.* **249,** 6416–6423.
17. Favreau, L. V. & Pickett, C. B. (1993) *J. Biol. Chem.* **268,** 19875–19881.
18. Jaiswal, A. K. (1994) *J. Biol. Chem.* **269,** 14502–14508.
19. Prestera, T., Prochaska, H. J. & Talalay, P. (1992) *Biochemistry* **31,** 824–833.
20. Suttie, J. W. (1980) *CRC Crit. Rev. Biochem.* **8,** 191–223.
21. Kabsch, W. (1988) *J. Appl. Crystallogr.* **21,** 67–71.
22. Kabsch, W. (1988) *J. Appl. Crystallogr.* **21,** 916–924.
23. *SERC* (1979) CCP4: *Collaborative Computing Project No. 4* (Daresbury Lab., Warrington, U.K.).
24. Wang, B.-C. (1985) *Methods Enzymol.* **115,** 90–112.
25. Boyington, J. C., Gaffney, B. J. & Amzel, L. M. (1993) *Science* **260,** 1482–1486.
26. Jones, T. A. (1978) *J. Appl. Crystallogr.* **11,** 268–272.
27. Sack, J. S. (1988) *J. Mol. Graphics* **6,** 244–249.
28. Brünger, A. T., Kuriyan, J. & Karplus, M. (1987) *Science* **235,** 458–460.
29. Evans, S. V. (1993) *J. Mol. Graphics* **11,** 134–138.
30. Chen, S., Deng, P. S. K., Bailey, J. M. & Swiederek, K. M. (1994) *Protein Sci.* **3,** 51–57.
31. Smith, W. W., Burnett, R. M., Darling, G. D. & Ludwig, M. L. (1977) *J. Mol. Biol.* **117,** 195–225.
32. Snow, M. E. & Amzel, L. M. (1986) *Proteins* **1,** 267–279.
33. Chen, S., Clarke, P. E., Martino, P. A., Deng, P. S. K., Yeh, C.-H., Lee, T. D., Prochaska, H. J. & Talalay, P. (1994) *Protein Sci.* **3,** 1296–1304.
34. Ma, Q., Cui, K., Xiao, F., Lu, A. Y. H. & Yang, C. S. (1992) *J. Biol. Chem.* **267,** 22298–22304.
35. Liu, X.-F., Yuan, H., Haniu, M., Iyanagi, T., Shively, J. E. & Chen, S. (1989) *Mol. Pharmacol.* **35,** 818–822.
36. Sem, D. S. & Kasper, C. B. (1992) *Biochemistry* **31,** 3391–3398.
37. Lee, C.-P., Simard-Duquesne, N., Ernster, L. & Hoberman, H. D. (1965) *Biochim. Biophys. Acta* **105,** 397–409.
38. Tedeschi, G., Chen, S. & Massey, V. (1995) *J. Biol. Chem.* **270,** 2512–2516.